

# Supporting material

Papaioannou A.,<sup>†</sup> Louis M.,<sup>‡</sup> Dhital B.,<sup>†</sup> Ho H. P.,<sup>‡</sup> Chang E. J.,<sup>‡</sup> and Boutis G.

S.<sup>\*,†,¶</sup>

*The Graduate Center of the City University of New York, Department of Physics, New York, New York, York College of The City University of New York, Department of Chemistry, Jamaica, New York, and Brooklyn College of The City University of New York, Department of Physics, Brooklyn, New York*

E-mail: [gboutis@brooklyn.cuny.edu](mailto:gboutis@brooklyn.cuny.edu)

---

\*To whom correspondence should be addressed

<sup>†</sup>The Graduate Center of the City University of New York, Department of Physics, New York, New York

<sup>‡</sup>York College of The City University of New York, Department of Chemistry, Jamaica, New York

<sup>¶</sup>Brooklyn College of The City University of New York, Department of Physics, Brooklyn, New York

# Theory

## Spin Interactions

Below we provide an overview of the salient spin physics used to probe elastins' dynamical characteristics by  $^{13}\text{C}$  magic angle spinning (MAS) NMR<sup>1-3</sup>. In a strong magnetic field the interaction Hamiltonian of the  $^{13}\text{C}$  nuclear spin system may be written,

$$\hat{\mathcal{H}}_{total} = \hat{\mathcal{H}}_{ij}^{DD} + \hat{\mathcal{H}}_{CS}. \quad (1)$$

In the above expression  $\hat{\mathcal{H}}_{ij}^{DD}$  is the heteronuclear dipole-dipole interaction between two interacting carbon and proton spins  $i$  and  $j$  and is written,

$$\hat{\mathcal{H}}_{ij}^{DD} = c_D(1 - 3\cos^2\theta_{ij})(3\hat{I}_{zi}\hat{S}_{zj} - \hat{I}_i \cdot \hat{S}_j). \quad (2)$$

In the above expression  $\theta$  is the angle between the internuclear axis and the static field  $B_0$ . The constant  $c_D$  is the dipole-dipole coupling constant, given by  $c_D = \frac{\gamma_i\gamma_j\hbar}{r_{ij}^3}[\frac{\mu_0}{4\pi}]$  in units of  $rad/s$ ,  $\gamma$  is the nuclear gyromagnetic ratio and  $\hbar$  is Planck's constant divided by  $2\pi$ . The second term in  $\hat{\mathcal{H}}_{total}$  is the chemical shielding Hamiltonian and is written,

$$\hat{\mathcal{H}}_{CS} = -\gamma\hbar\vec{I} \cdot \vec{\sigma} \cdot \vec{B}_0, \quad (3)$$

where  $\vec{I}$  is the carbon nuclear spin operator,  $\vec{B}_0$  is the static field,  $\vec{\sigma}$  is the chemical shift tensor and  $\vec{B}_0$  is the Zeeman field. Only the diagonal elements of  $\vec{\sigma}$  which correspond to the isotropic chemical shift affect the NMR spectrum whereas the off-diagonal elements of  $\vec{\sigma}$  vanish under MAS conditions. Additionally, under high power  $^1\text{H}$  decoupling, the heteronuclear dipole-dipole interaction between  $^1\text{H}$  and  $^{13}\text{C}$  nuclei vanishes, allowing for a measurement of the

isotropic chemical shift interaction.

## NMR Relaxation

The time dependent nature of a fluctuating magnetic field  $B(t)$  may be generally described by a two point autocorrelation function which is written

$$\mathcal{G}(t_1, t_2) = \langle B(t_1)B(t_2) \rangle, \quad (4)$$

relative to times  $t_1$  and  $t_2$ . Because  $\mathcal{G}(t_1, t_2)$  is time invariant one may define the time  $\tau = t_1 - t_2$ . The Fourier transform of the autocorrelation function is defined as

$$\mathcal{J}_n(\omega) = \frac{1}{\sqrt{2\pi}} \int_0^\infty \mathcal{G}_n(\tau) e^{-i\omega\tau} d\tau \quad n = 0, 1, 2, \dots, \quad (5)$$

where  $\mathcal{J}(\omega)$  is the spectral density function given by<sup>4,5</sup>

$$\mathcal{J}_n(\omega) = \frac{2}{5}(1 - S^2) \frac{\tau_c}{1 + (\tau_c\omega)^2}. \quad (6)$$

In the above expression  $S^2$  is the order parameter which describes motional restriction and  $\tau_c$  is the correlation time of all  $^1\text{H}$ - $^{13}\text{C}$  internuclear vectors; a reduction in the correlation time denotes faster tumbling of the  $^1\text{H}$ - $^{13}\text{C}$  internuclear vectors.

The spin-lattice relaxation rate in the rotating frame for two different spins I, S may be written in terms of the spectral densities  $\mathcal{J}_n(\omega)$  as,

$$R_{IS}^{1\rho} = \mu_S^2 \left\{ \frac{1}{2} \left[ \mathcal{J}_0(\omega_I - \omega_S) + 3\mathcal{J}_1(\omega_I) + \mathcal{J}_2(\omega_I + \omega_S) \right] \right\} + R_{1\Delta}^{IS} \quad (7)$$

where,

$$R_{1\Delta}^{IS} = \mu_S^2 \left\{ 3\mathcal{J}_1(\omega_S) + \frac{1}{3} [\mathcal{J}_0(\omega_e - 2\omega_R) + \mathcal{J}_0(\omega_e + 2\omega_R)] + \frac{2}{3} [\mathcal{J}_0(\omega_e - \omega_R) + \mathcal{J}_0(\omega_e + \omega_R)] \right\}. \quad (8)$$

In the above expressions  $\omega_e$  is the frequency of the spin locking field (which is applied to the  $^{13}\text{C}$  nuclei in our study)  $\omega_R$  is the spinning frequency of the rotor,  $\mu_s^2 = c_D^2/4$  and  $\omega_I$  and  $\omega_S$  are the Larmor frequencies of the  $^1\text{H}$  and  $^{13}\text{C}$  spins respectively<sup>4</sup>. The dipolar coupling constant,  $c_D$ , should be interpreted as the average dipolar interaction constant of a single carbon with the surrounding  $^1\text{H}$  spins.

In the limit of fast and isotropic molecular motion, the order parameter  $S^2$  that describes the anisotropy of the motion is approximately zero, and the spectral density reduces to,

$$\mathcal{J}(\omega) = \mathcal{J}_n(\omega) = \frac{2}{5} \frac{\tau_c}{(1 + \tau_c^2 \omega^2)} \quad n = 0, 1, 2, 3, \dots \quad (9)$$

In the above theoretical approach one effective  $^1\text{H}$ - $^{13}\text{C}$  internuclear vector is assumed and is approximated by a single correlation time<sup>4,5</sup>. Measurement of the transverse relaxation time  $T_{1\rho}$  at two different locking fields  $\omega_e$  and  $\omega'_e$ , allows for the determination of the average correlation time  $\tau_c$  described above<sup>6</sup>.

# Results and Discussion

## Dynamical and structural characteristics of hydrated elastin

Figure 2 of the main text show the direct polarization (DP) and cross polarization (CP)  $^{13}\text{C}$  NMR spectra of hydrated bovine nuchal ligament elastin purified by the autoclaving method at 37°C (Sample 1). The chemical shift assignment was performed following standard chemical shift tables<sup>7,8</sup> by converting all the spectra to TMS scale<sup>9</sup>. One of the models proposed for the secondary structure of elastin is characterized by  $\beta$ -strand/ $\beta$ -sheet and random coil secondary structures<sup>10</sup>. Our overall experimental results on the hydrated samples appear to generally agree with this finding as we observe more  $\beta$ -strand and random coil like motifs in the  $^{13}\text{C}$  NMR spectrum as discussed below. The measured chemical shifts and the structural assignments are shown and compared with known random coil,  $\alpha$ -helix and  $\beta$ -strand chemical shifts in Table 2.

The backbone carbonyl carbons at 172.1ppm show a splitting, but our spectral resolution does not permit a detailed assignment or decomposition of the signal. Additionally, the relative signal intensity of the backbone carbonyl in the DP experiment (Figure 2a) is increased in comparison with that in the CP experiment (Figure 2c). As discussed above, reduced signal intensity in the cross polarization experiments indicates fast and isotropic motion, revealing high mobility of the backbone carbonyl. In addition, a reduction of the signal intensity of the CP experiment may emerge from the absence of directly bound hydrogens. The broad peak at 129.0ppm was assigned to the aromatic carbons of phenylalanine and tyrosine as previously reported by Kumashiro and coworkers<sup>11</sup>. In the aliphatic region the highest intensity peaks at approximately 18.0ppm and 19.0ppm were assigned to alanine- $C_\beta$  and valine- $C_\gamma$  respectively. According to<sup>7,8,12</sup> these chemical shifts would appear to point to random coil and  $\beta$ -strand motifs. Previous studies performed by Wittebort et al. reported that the alanine moieties of elastin may be in a random coil configuration<sup>13</sup>. Additionally, Kumashiro et al. reported that this chemical shift in  $\alpha$ -elastin might result

from  $\beta$ -structure<sup>11</sup>. Another important observation that needs to be noted here is that the two peaks at 18.0ppm and 19.0ppm are quite well resolved in both DP and CP experiments, indicating slow or anisotropic motion of these moieties. Slightly more upfield, the signal at 22.0ppm may also correspond to alanine- $C_\beta$ . This chemical shift would point to  $\beta$ -strand conformation. Keeley and coworkers reported that poly-alanine motifs in elastin include domains such as (AAAAA), (AAKAA) and (GAG)<sup>14</sup>. It has been observed by Buehler and Keten that similar polyalanine regions found in dragline silks form  $\beta$ -sheet structures<sup>15</sup>, and more recently, it has been shown that the  $\beta$ -sheet structures are unaffected even when the silk is hydrated<sup>16</sup>. Additionally, the (GAG) motifs of elastin were found to form a  $3_1$ -helices in silk<sup>15,17</sup>.

The isoleucine- $C_\gamma$  and - $C_\delta$  signals appear at approximately 11.0ppm and 16.0ppm, respectively, but no further secondary structure assignments can be made. Leucine- $C_\delta$  and proline- $C_\gamma$  were observed at approximately 23.5ppm and 25.6ppm. The peak at 31.0ppm was assigned to proline- $C_\beta$ , in agreement with other studies<sup>11,18,19</sup> and within our experimental uncertainty this chemical shift points to either random coil,  $\alpha$ -helical or  $\beta$ -strand structures. Additionally, the valine- $C_\beta$  signal overlaps with the proline- $C_\beta$  signal and would indicate either  $\beta$ -strand, random coil or  $\alpha$ -helical structure. These experimental observations appear to correlate with the Ramachandran maps at 42°C of (VPGVG)<sub>18</sub><sup>20</sup> and (VPGVG)<sub>3</sub><sup>21</sup> in MD simulation. The peak at 37.0ppm was assigned to isoleucine- $C_\beta$ . In previous studies, isoleucine rich motifs were found to be in more random coil structure having a chemical shift of approximately 39.0ppm (TMS scale)<sup>13</sup>, but our measurement points to  $\beta$ -strand in addition to random coil structure rather than one structural motif<sup>7</sup>.

Previous NMR studies on elastin reported a glycine- $C_\alpha$  chemical shift of 43ppm<sup>11</sup>. In addition, the same group performed <sup>13</sup>C-NMR and <sup>15</sup>N-NMR studies on glycine enriched elastin and reported that it is rather ambiguous to make any secondary structure assignments due to the fact that glycine- $C_\alpha$  <sup>13</sup>C chemical shifts of  $\beta$ -turn,  $3_1$ -helix and  $\alpha$ -helical secondary structures are nearly the same<sup>22</sup>. The measured chemical shift of the glycine- $C_\alpha$  carbons in

our study was 43.4ppm. Asakura et al. studied the structure of glycine rich motifs in various proteins<sup>23</sup>. According to their findings our observed glycine chemical shift would appear to be to have  $\alpha$ -helical secondary structure. On the other hand studies of dragline silk, such as that from *N. Clavipes*, have reported  $\beta$ -sheet motifs for the same chemical shift observed in our experiments<sup>24</sup>. Thus, the exact secondary structure assignment of glycine rich motifs of elastin still remains rather unclear. Lastly, we observe a notable difference in the relative signal intensities of glycine in the DP and CP experiments shown in Figure 2; this indicates that glycine rich moieties of elastin are rather mobile. The high mobility of glycine motifs in elastin has also been discussed elsewhere<sup>25</sup>.

The peaks at 48.0ppm and 51.0ppm were assigned to alanine- $C_\alpha$  with  $\beta$ -strand and random coil secondary structures, in agreement with our previous noted assignment of the alanine- $C_\beta$ . In addition, the peak at 51.0ppm was assigned to the proline- $C_\delta$ . The peak at 53.3ppm was also assigned to the alanine- $C_\alpha$  and this chemical shift points to  $\alpha$ -helical conformations. Therefore, the alanine motifs of elastin seem to exhibit a heterogeneity of structures according to our measured chemical shifts. In addition, the phenylalanine  $C_\alpha$  chemical shift also appears at 53.3ppm and this chemical shift points to  $\beta$ -strand secondary structure.

The valine- $C_\alpha$  signal was observed at approximately 60.4ppm and within our experimental uncertainty this chemical shift points to  $\beta$ -strand and random coil like structures<sup>7</sup>. Wittebort and his group reported valine motifs took up a random coil secondary structure based on the chemical shift of the  $C_\alpha$ <sup>13</sup>. It should be noted that the proline- $C_\alpha$  signal contributes non-negligibly to the peak at 60.4ppm corresponding to  $\beta$ -strand or random coil structures. Previous studies showed that proline- $C_\alpha$  appears in random coil secondary structure<sup>13</sup>. In addition, the torsion angles derived from short MD simulations of  $(VPGVG)_{18}$  and  $(VPGVG)_3$  showed the presence of  $\beta$ -turns<sup>20,21</sup>.

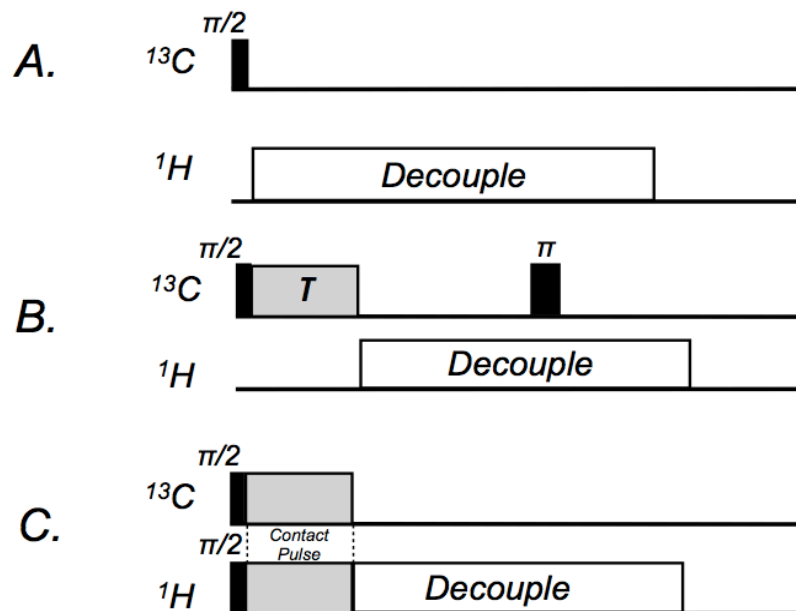


**Figure S2:** NMR pulse sequences implemented in this work. A) Direct polarization (DP) pulse sequence, B) pulse sequence for measuring the  $^{13}\text{C}$   $T_{1\rho}$  relaxation time and C) cross polarization pulse sequence. In sequence B the amplitude of the applied spin locking field on the carbon channel is varied between two settings and as discussed in the text, a  $\pi$  pulse was used to reduce the effects of ring down artifacts. In C, for cross polarization (CP) a contact pulse of 3ms was used. Other experimental parameters are discussed further in the methods section of the manuscript.



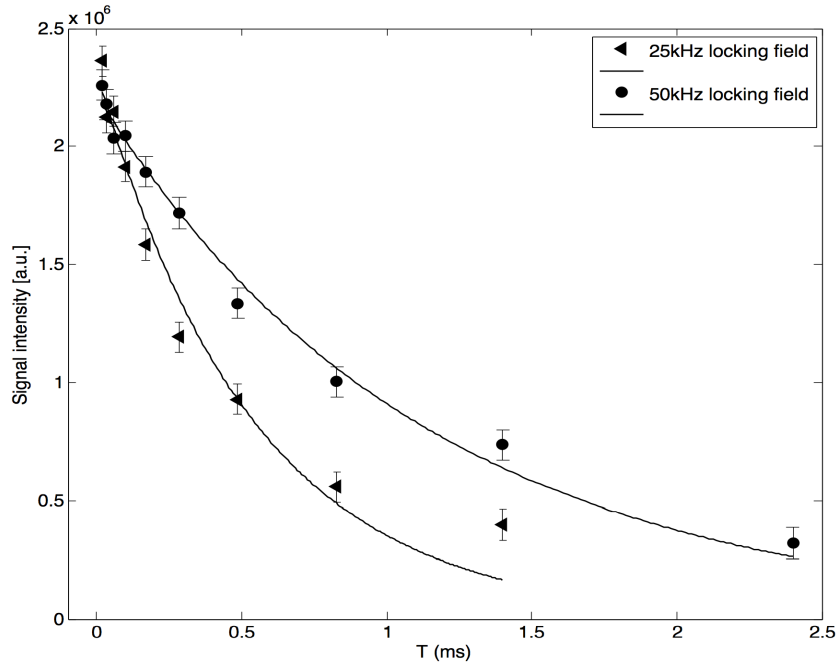


**Figure S1:** Sample  $T_{1\rho}$  relaxation curves of proline- $C_\beta$  of hydrated elastin (sample 1) purified by the autoclaving method. The experimental data were fit to a single exponential with  $\chi^2/dof = 1.22$  (50kHz) and  $\chi^2/dof = 4.33$  (25kHz). As described in the text, determination of the spin-lattice relaxation rate in the rotating frame, at two different spin locking fields allows for the determination of the correlation time  $\tau_c$ .

## References

- (1) Abragam, A. *Principles of Nuclear Magnetism (International Series of Monographs on Physics)*; Oxford University Press, USA, 1983.
- (2) Duer, M. J. *Introduction to Solid-State NMR Spectroscopy*; Wiley-Blackwell, UK, 2005.
- (3) Slichter, C. *Principles of Magnetic Resonance*; Springer, USA, 1996.
- (4) Kurbanov, R.; Zinkevich, T.; Krushelnitsky, A. *The Journal of Chemical Physics* **2011**, *135*, 184104.
- (5) Lipari, G.; Szabo, A. *Journal of the American Chemical Society* **1982**, *104*, 4546–4559.
- (6) Yao, X. L.; Conticello, V. P.; Hong, M. *Magnetic Resonance in Chemistry* **2004**, *42*, 267–75.
- (7) Zhang, H.; Neal, S.; Wishart, D. S. *Journal of Biomolecular NMR* **2003**, *25*, 173–95.
- (8) Wang, Y.; Jardetzky, O. *Protein Science* **2002**, *11*, 852–861.
- (9) Wishart, D. S.; Bigam, C. G.; Yao, J.; Abildgaard, F.; Dyson, H. J.; Oldfield, E.; Markley, J. L.; Sykes, B. D. *Journal of Biomolecular NMR* **1995**, *6*, 135–140.
- (10) Debelle, L.; Alix, A. J. *Biochimie* **1999**, *81*, 981–94.
- (11) Kumashiro, K. K.; Kim, M. S.; Kaczmarek, S. E.; Sandberg, L. B.; Boyd, C. D. *Biopolymers* **2001**, *59*, 266–75.
- (12) Cavanagh, J.; Fairbrother, W. J.; Palmer III, A. G.; Skelton, N. J. *Protein NMR spectroscopy: principles and practice*; Academic Press, 1995.
- (13) Pometun, M. S.; Chekmenev, E. Y.; Wittebort, R. J. *The Journal of Biological Chemistry* **2004**, *279*, 7982–7.

- (14) He, D.; Chung, M.; Chan, E.; Alleyne, T.; Ha, K. C.; Miao, M.; Stahl, R. J.; Keeley, F. W.; Parkinson, J. *Matrix Biology* **2007**, *26*, 524–540.
- (15) Keten, S.; Buehler, M. J. *Journal of the Royal Society Interface* **2010**, *7*, 1709–1721.
- (16) Holland, G. P.; Jenkins, J. E.; Creager, M. S.; Lewis, R. V.; Yarger, J. L. *Biomacromolecules* **2008**, *9*, 651–657.
- (17) Ashida, J.; Ohgo, K.; Komatsu, K.; Kubota, A.; Asakura, T. *Journal of Biomolecular NMR* **2003**, *25*, 91–103.
- (18) Lusceac, S. A.; Vogel, M. R.; Herbers, C. R. *Biochimica et Biophysica acta. Proteins and Proteomics* **2010**, *1804*, 41–48.
- (19) Kumashiro, K. K.; Ho, J. P.; Niemczura, W. P.; Keeley, F. W. *The Journal of Biological Chemistry* **2006**, *281*, 23757–65.
- (20) Li, B.; Alonso, D. O.; Daggett, V. *Journal of Molecular Biology* **2001**, *305*, 581–92.
- (21) Huang, J.; Sun, C.; Mitchell, O.; Ng, N.; Wang, Z. N.; Boutis, G. S. *The Journal of Chemical Physics* **2012**, *136*, 085101.
- (22) Perry, A.; Stypa, M. P.; Foster, J. a.; Kumashiro, K. K. *Journal of the American Chemical Society* **2002**, *124*, 6832–3.
- (23) Asakura, T.; Iwadate, M.; Demura, M.; Williamson, M. P. *International Journal of Biological Macromolecules* **1999**, *24*, 167–71.
- (24) Jenkins, J. E.; Creager, M. S.; Lewis, R. V.; Holland, G. P.; Yarger, J. L. *Biomacromolecules* **2010**, *11*, 192–200.
- (25) Perry, A.; Stypa, M. P.; Tenn, B. K.; Kumashiro, K. K. *Biophysical Journal* **2002**, *82*, 1086–95.